J Am Chem Soc. Author manuscript; available in PMC 2014 October 30.

Published in final edited form as:

J Am Chem Soc. 2013 October 30; 135(43): . doi:10.1021/ja405993r.

# Membrane Remodeling by $\alpha$ -Synuclein and Effects on Amyloid Formation

#### Zhiping Jiang, Michel de Messieres, and Jennifer C. Lee\*

Laboratory of Molecular Biophysics, Biochemistry and Biophysics Center, National Heart, Lung, and Blood Institute, National Institutes of Health, Bethesda, MD 20892, United States

### **Abstract**

α-Synuclein (α-Syn), an intrinsically disordered protein, is associated with Parkinson's disease. Though molecular pathogenic mechanisms are ill-defined, mounting evidence connects its amyloid forming and membrane binding propensities to disease etiology. Contrary to recent data suggesting that membrane remodeling by α-syn involves anionic phospholipids and helical structure, we discovered that the protein deforms vesicles with no net surface charge (phosphatidylcholine, PC) into tubules (average diameter ~ 20 nm). No discernible secondary structural changes were detected by circular dichroism spectroscopy upon the addition of vesicles. Notably, membrane remodeling inhibits α-syn amyloid formation affecting both lag and growth phases. Using five single-tryptophan variants and time-resolved fluorescence anisotropy measurements, we determined that α-syn influences bilayer structure with surprisingly weak interaction and no site specificity (partition constant,  $K_p \sim 300 \, \mathrm{M}^{-1}$ ). Vesicle deformation by α-syn under a variety of different lipid/protein conditions is characterized *via* transmission electron microscopy. As cellular membranes are enriched in PC lipids, these results support possible biological consequences for α-syn induced membrane remodeling related to both function and pathogenesis.

 $\alpha\textsc{-Synuclein}\ (\alpha\textsc{-syn}),$  an intrinsically disordered protein, is enriched in the presynaptic nerve terminals. Intracellular accumulation of  $\alpha\textsc{-syn}$  amyloid is a histopathological hallmark of Parkinson's disease (PD). Missense mutations of  $\alpha\textsc{-syn}$ , as well as gene duplication and triplication, are linked to familial, early-onset PD, implicating the protein as a pathogenic agent. While its biological function is ill-defined, various data suggest that  $\alpha\textsc{-syn}$  association with synaptic vesicles plays a role in neuronal transmission. Importantly, mounting evidence supports aberrant  $\alpha\textsc{-syn-membrane}$  interactions in cytotoxicity, including Golgi fragmentation, mitochondrial fission, and lysosomal malfunction. Molecular mechanisms by which  $\alpha\textsc{-syn}$  promotes membrane disruption are not well understood.

An emerging view is that  $\alpha$ -syn can strongly influence the structure and properties of phospholipid bilayers. Recent examples include membrane thinning, <sup>6</sup> membrane curvature generation, <sup>7</sup> as well as formation of tubular structures. <sup>8</sup> Presence of anionic phospholipids, *e.g.* phosphatidylglycerol (PG), phosphatidylserine, or phosphatidic acid (PA), and folding of  $\alpha$ -helical structure are thought to be essential for membrane binding and remodeling (deformation) by  $\alpha$ -syn. Membrane shapes along with bilayer integrity are crucial in cellular activities such as intracellular vesicular transport. <sup>9</sup> Accordingly, it is compelling to

<sup>\*</sup>Corresponding Author: leej4@mail.nih.gov.

The authors declare no competing financial interests.

Supporting Information

hypothesize that  $\alpha$ -syn bends and remodels membranes as part of its physiological as well as pathological function.

In prior work using neutron reflectivity measurements, we have shown that  $\alpha$ -syn partially inserts into the outer leaflet of the bilayer and thins the membrane. This observation is consistent with a "wedge" model ascribed to other known curvature-generating proteins: the hydrophobic insertion of an amphipathic  $\alpha$ -helix acts as a wedge, pushing phospholipid headgroups apart, inducing thinning and spontaneous local curvature. Here, we aim to understand how membrane remodeling by  $\alpha$ -syn affects the fibril formation process.

Since negatively charged lipids are considered important for membrane tubulation,  $^{8a,8b}$  we selected phosphatidylcholine, (palmitoyl-2-oleoyl-sn-glycero-3-phosphocholine, POPC), a zwitterionic and the most abundant phospholipid in all mammalian membranes, as a negative control. Negative staining and transmission electron microscopy (TEM) were employed to visualize and assess vesicle morphology. Most unexpectedly, unilamellar POPC vesicles were significantly remodeled upon addition of  $\alpha$ -syn (Figure 1 and S1). In the absence of  $\alpha$ -syn, minimal vesicle deformation is observed (Figure 1A). As  $\alpha$ -syn is added, vesicle remodeling is apparent with buds forming at the submicromolar regime (Figure 1B). At higher protein concentrations, tubulation occurs (Figure 1C, 1D). Analysis of TEM images yielded the fraction of tubule area formed as a function of  $\alpha$ -syn concentration (Figure 1E, Table S1). With increasing  $\alpha$ -syn, more tubulation is observed. POPC tubulation by  $\alpha$ -syn (5  $\mu$ M) is also seen at varying lipid concentrations (Figure S2).

POPC tubule structures induced by  $\alpha$ -syn are wider (average diameter =  $20 \pm 5$  nm) compared to that of previously reported cylindrical micelles formed from POPG multilamellar vesicles (MLVs). Sa,8b Lipid tubules formed from sonicated POPG vesicles have similar widths to those formed from MLVs (7  $\pm$  3 nm, Figure S3). To directly compare and to exclude the effect of vesicle preparation methods, POPC MLVs as well as extruded POPC vesicles (100 nm pore size) were examined. Tubules are observed independent of lipid preparation (Figure S4). While tubules are formed with POPC lipids, they occur with less efficiency compared to POPG (Figure S5). Deformed POPC MLVs appear somewhat intact with tubules emanating from them. Unlike the POPG tubules, these structures would scatter significant amounts of light and thus not become optically clear upon the addition of  $\alpha$ -syn. Sa

To detect secondary structural changes of  $\alpha$ -syn in the presence of POPC vesicles, far-UV circular dichroism (CD) spectroscopy was employed. In solution,  $\alpha$ -syn is highly disordered with a characteristic negative maximum near 200 nm. No discernible spectral changes are observed upon the addition of vesicles (Figure 1F), indicating that the protein remains unfolded (See Table S2 for deconvolution results). While these results are suggestive that unstructured  $\alpha$ -syn is capable of transforming vesicles with no net surface charge into tubules, these measurements do have their associated detection limits and do not preclude the existence of low amounts of helical structure. Moreover, they are made at equilibrium and therefore do not address structural changes that may occur under non-equilibrium conditions which may be the case for membrane tubulation.

As the interaction region between  $\alpha$ -syn and POPC vesicles is unknown and generally considered non-existent<sup>11</sup> or ill-defined, <sup>12</sup> we employed five single-Trp variants<sup>13</sup> (F4W, Y39W, F94W, Y125W and Y136W) and time-resolved fluorescence anisotropy measurements to probe for association through Trp side-chain mobility. In buffer, all Trp sites show similar kinetics where ~90% of the Trp fluorescence depolarizes rapidly ( 150 ps) and the residual anisotropy ( $r_0 = 0.06$ ) decays to zero (0.8-ns time constant, Figure 2A), consistent with an unfolded polypeptide. <sup>14</sup> Upon the addition of POPC vesicles,  $r_0$  for all

Trp sites increases (0.16) and does not fully decay to zero, indicating that a subpopulation of Trp sidechains is highly restricted due to membrane interaction.

No site dependence is discernible upon association with POPC vesicles. This is unanticipated because it is well known that the first 100 residues constitute the helical, membrane binding region while the last 40 C-terminal, acidic residues remain disordered and water-exposed. However, it had been proposed that the glutamate-rich C-terminal region (120–140), rather than the N-terminal portion, interacts with the positively charged choline headgroups. Thus, it is reasonable to expect some differences amongst the Trp sites. While our data suggest nonspecific lipid interaction throughout the polypeptide chain, the lack of residue specificity may also be explained by the general restriction of intrachain diffusion on the bilayer. Nevertheless, as  $r_0$  value increases with increasing concentrations of POPC, a binding curve can be obtained (Figure 2B). The data were fit to yield a partition constant,  $K_p \sim 300~\text{M}^{-1}$ , confirming weak binding as previously reported,  $^{12a} \sim 14$  times smaller than that obtained for POPC/POPA.

Because there is no apparent specific region for interaction, we tested whether different regions of the protein could induce membrane remodeling. Both truncation (1–60 and 96–140) and deletion ( $\Delta 61$ –95)  $\alpha$ -syn variants were able to reshape POPC vesicles (Figure S7). This phenomenon appears to be a general property of the synuclein family as the other homologous members,  $\beta$ - and  $\gamma$ -syn, also bend and reshape vesicles. As a negative control, the addition of bovine serum albumin, a standard protein used to model nonspecific interaction, does not influence membrane structure (Figure S7). Finally, we establish that N-terminally acetylated  $\alpha$ -syn also remodels POPC vesicles (Figure S7) since it is now known that the majority of protein is acetylated *in vivo* and this post-translational modification enhances membrane interactions *in vitro*. <sup>17</sup>

Insertion of a short helix (< 11 residues as estimated by CD data) with minimal surface coverage (~0.2%) is unlikely to generate the observed tubule width according to the hydrophobic insertion model. <sup>18</sup> So, how does a disordered protein deform vesicles? We hypothesize that upon protein binding, a local enrichment of  $\alpha$ -syn molecules causes an asymmetric stress to the outer leaflet, initiating spontaneous curvature generation. Rather than embedding of a small helix at or below the phosphate level, interactions of the disordered 140-residue  $\alpha$ -syn near the choline region would hypothetically impart adequate inclusion area to cause membrane tubulation. The surface area coverage for unstructured  $\alpha$ -syn is estimated at ~21–27% (L/P = 300), which is sufficient for spontaneous curvature generation with shallow penetration (2–3 Å) from the lipid surface. <sup>18</sup>

This proposal may explain why POPC bending by  $\alpha\text{-syn}$  is weaker than what has been observed for POPG which results from a deeper insertion of an extended helix (> 63% helical content). Alternatively,  $\alpha\text{-syn}$  induced POPC tubulation may occur via the mechanism of protein-protein crowding where with sufficient surface coverage ( 20%), membranes are bent with proteins concentrating at the membrane surface.  $^{19}$  Clearly, to elucidate the mechanism of POPC membrane tubulation by  $\alpha\text{-syn}$ , further characterization is needed including determination of lipid tubule structure and the location of  $\alpha\text{-syn}$  on these structures.

To gain insights from the lipid perspective, we examined two other vesicle compositions incorporating cholesterol (Chol) or POPA into POPC vesicles. The addition of Chol, a vital structural molecule of cellular membranes, should suppress curvature generation as the bilayer becomes more ordered and rigid. We also reasoned that despite its high propensity to induce  $\alpha$ -syn helical structure, <sup>13</sup> the preference for negative curvature of the small PA headgroup will likely attenuate membrane tubulation. As predicted,  $\alpha$ -syn induced

tubulation of POPC/Chol (3:2) and POPC/POPA (1:1) vesicles is reduced and non-existent, respectively (Figure S8). Effects of Chol on vesicle remodeling of POPC by  $\alpha$ -syn are quantified in Figures S9 and S10 as well as in Table S3. Differences in membrane remodeling are not attributable to binding affinities as  $\alpha$ -syn binding to POPC/Chol vesicles ( $K_p \sim 200~\text{M}^{-1}$ , Figure 2B) is comparable to POPC alone. For POPC/POPA vesicles, helical formation does not induce membrane tubulation. Using a supported bilayer, another study found that tubulation is minimized with increasing POPA concentration. <sup>8e</sup>

With establishment of lipid compositions that support and prevent membrane remodeling, we measured the effect of tubule (POPC) and non-tubule forming (POPC/POPA) lipid vesicles on  $\alpha$ -syn fibril formation kinetics. Aggregation experiments were performed in the absence and presence of varying amounts of vesicles and monitored by thioflavin T (ThT) fluorescence (Figure 3A). After reaching stationary phase,  $\beta$ -sheet and fibril structure are characterized by CD spectroscopy and TEM, respectively (Figure 3B–I).

Highly divergent behaviors are evident for the two lipid compositions, affecting both lag and growth phases. The presence of POPC vesicles slows α-syn aggregation. Notably, ThT intensity is decreased as POPC vesicles are increased, suggesting either amyloid formation is reduced or that the aggregates are substantially less ThT-active. CD data are consistent with the reduction of amyloid formation as the presence of β-sheet structure is decreased compared to α-syn fibrils formed in buffer alone (Figure 3B). In contrast, the lag phase is shortened and the growth rate is accelerated in the presence of POPC/POPA vesicles. Formation of a partially helical structure (~13% helicity, L/P = 50) in POPC/POPA stimulates fibril formation, consistent with prior work. The mechanism of POPC/POPA enhancement of α-syn aggregation remains to be elucidated. It is possible that concentration of a few α-syn molecules, and/or formation of transient α-helix intermediates at the membrane interface, facilitates protein-protein interactions, forming a nucleation site for recruitment of other α-synucleins, and thereby enhancing the aggregation process.

No distinctive morphological differences between the filaments formed under the different solution conditions are observed by TEM (Figure 3). However, POPC vesicles are clearly deformed. Consistent with ThT data, fewer fibrils are seen in the presence of more POPC vesicles. Instead, tubules are present and dominate at higher L/P (Figure 3F), implying that the two structures compete for the available pool of free  $\alpha$ -syn. POPC remodeling by  $\alpha$ -syn appears to be independent of relative rate of aggregation as consistent results were obtained at acidic pH (5.0), a solution condition known to facilitate oligomerization and fibril formation (Figure S11).  $^{22}$ 

When preformed  $\alpha$ -syn filaments are added to POPC vesicles, no membrane restructuring is observed (Figure 3G). All vesicles are circular and intact, suggesting that monomers, rather than fibrils, remodel membranes. Our data do not rule out the possibility of membrane deformation by  $\alpha$ -syn oligomers or intermediates populated during aggregation. The involvement of oligomers is plausible as shown in two recent studies. One suggested that helical  $\alpha$ -syn oligomers transform POPG vesicles into ellipsoidal nanoparticles. <sup>23</sup> The other showed that  $\alpha$ -syn, removed during the lag-phase, forms tube-like structures when added to PC membranes, <sup>24</sup> though these structures were interpreted to be radiating  $\alpha$ -syn amyloid fibrils and not deformed membranes. Since monomers do remodel POPC membranes (Figure 1), we favor activity by the monomer, which explains the observed inhibition of amyloid formation where monomers are sequestered from aggregation.

In contrast to POPC, POPC/POPA vesicles remain intact during α-syn aggregation (Figure 3H, I). No obvious tubular structures are observed. While the presence of lipid tubules cannot be completely excluded as differences in filament *vs.* tubule morphology may be

difficult to discern, ThT and CD data support that amyloid fibrils are prevalent. Many fibrils appear to associate with vesicles. It could be inferred that the membrane serves as aggregation initiation sites or simply that the fibrils themselves have some affinity for the membrane surface. Both cases are plausible as POPC/POPA vesicles strongly influence  $\alpha$ -syn aggregation and preformed amyloids also appear to adhere to POPC vesicles (Figure 3G).

In summary,  $\alpha$ -syn directly remodels and tubulates zwitterionic POPC membranes. Strikingly,  $\alpha$ -syn deforms POPC vesicles through weak interactions (estimated dissociation constant,  $K_d \sim \text{mM}$ ), which is unusual for membrane curvature generating proteins such as amphiphysin 1 and BAR domains where  $K_d$  values are in the range of tens to hundreds of nM.<sup>25</sup> This work suggests that membrane bending by  $\alpha$ -syn may be more complicated than the currently proposed amphipathic helix insertion model; however, more work is needed to evaluate whether other mechanisms are at play.  $\alpha$ -Syn mediates membrane curvature generation in concert with various lipids, suggesting that this ability may be of biological relevance. A recent study in mice with all three  $\alpha$ -,  $\beta$ - and  $\gamma$ -syn genes knocked out demonstrates enhanced levels of several BAR domain proteins, <sup>8d</sup> membrane curvature sensing/generating proteins, implying up-regulation to compensate the loss of function from synuclein deficiency. Other possibilities include  $\alpha$ -syn playing a role in synaptic vesicle fusion during neurotransmission.<sup>26</sup>

Finally, there also may be pathological connections for  $\alpha$ -syn induced membrane bending. For example,  $\alpha$ -syn overexpression results in excess  $\alpha$ -syn release and transmission through exosomes, a proposed pathway for intercellular exchange of material,  $^{27}$  supporting the controversial hypothesis that PD is a prion-like disease.  $^{28}$   $\alpha$ -Syn aggregation appears to be inhibited as a result of membrane remodeling, *i.e.*, more monomers involved in tubule formation so fewer proteins are available to form fibrils. In a healthy individual, lipid metabolism is tightly regulated but the balance changes with age.  $^{29}$  It is conceivable that subtle and/or local differences in membrane composition may lead to aberrant membrane deformation or enhance formation of cytotoxic aggregates, two distinct pathological outcomes.

## **Supplementary Material**

Refer to Web version on PubMed Central for supplementary material.

# **Acknowledgments**

Supported by the Intramural Research Program at the NIH, NHLBI. We thank the NHLBI EM, Biophysics, and Biochemistry Cores and Yi He for the use of equipment and technical expertise. We also thank Dan Mulvihill (University of Kent) for the gift of pNatB plasmid and Jian Liu (NHLBI) for helpful discussions.

#### References

- Spillantini MG, Schmidt ML, Lee VMY, Trojanowski JQ, Jakes R, Goedert M. Nature. 1997; 388:839–840. [PubMed: 9278044]
- 2. Lucking CB, Brice A. Cell Mol Life Sci. 2000; 57:1894–1908. [PubMed: 11215516]
- 3. Cheng FR, Vivacqua G, Yu S. J Chem Neuroanat. 2011; 42:242–248. [PubMed: 21167933]
- (a) Gosavi N, Lee HJ, Lee JS, Patel S, Lee SJ. J Biol Chem. 2002; 277:48984–48992. [PubMed: 12351643]
  (b) Fujita Y, Ohama E, Takatama M, Al-Sarraj S, Okamoto K. Acta Neuropathol. 2006; 112:261–265. [PubMed: 16855830]
  (c) Nakamura K, Nemani VM, Azarbal F, Skibinski G, Levy JM, Egami K, Munishkina L, Zhang J, Gardner B, Wakabayashi J, Sesaki H, Cheng YF, Finkbeiner S, Nussbaum RL, Masliah E, Edwards RH. J Biol Chem. 2011; 286:20710–20726. [PubMed:

- 21489994] (d) Meredith GE, Totterdell S, Petroske E, Cruz KS, Callison RC, Lau YS. Brain Res. 2002; 956:156–165. [PubMed: 12426058]
- 5. (a) Butterfield SM, Lashuel HA. Angew, Chem, Int Ed. 2010; 49:5628–5654.(b) Beyer K. Cell Biochem Biophys. 2007; 47:285–299. [PubMed: 17652776]
- Pfefferkorn CM, Heinrich F, Sodt AJ, Maltsev AS, Pastor RW, Lee JC. Biophys J. 2012; 102:613–621. [PubMed: 22325285]
- 7. Braun AR, Sevcsik E, Chin P, Rhoades E, Tristram-Nagle S, Sachs JN. J Am Chem Soc. 2012; 134:2613–2620. [PubMed: 22211521]
- (a) Varkey J, Isas JM, Mizuno N, Jensen MB, Bhatia VK, Jao CC, Petrlova J, Voss JC, Stamou DG, Steven AC, Langen R. J Biol Chem. 2010; 285:32486–32493. [PubMed: 20693280] (b) Mizuno N, Varkey J, Kegulian NC, Hegde BG, Cheng NQ, Langen R, Steven AC. J Biol Chem. 2012; 287:29301–29311. [PubMed: 22767608] (c) Taneva SG, Lee JMC, Cornell RB. BBA-Biomembranes. 2012; 1818:1173–1186. [PubMed: 22285779] (d) Westphal CH, Chandra SS. J Biol Chem. 2013; 288:1829–1840. [PubMed: 23184946] (e) Pandey AP, Haque F, Rochet JC, Hovis JS. J Phys Chem B. 2011; 115:5886–5893. [PubMed: 21520980]
- 9. Zimmerberg J, Kozlov MM. Nat Rev Mol Cell Biol. 2006; 7:9–19. [PubMed: 16365634]
- Baumgart T, Capraro BR, Zhu C, Das SL. Annu Rev Phys Chem. 2011; 62:483–506. [PubMed: 21219150]
- Davidson WS, Jonas A, Clayton DF, George JM. J Biol Chem. 1998; 273:9443–9449. [PubMed: 9545270]
- 12. (a) Middleton ER, Rhoades E. Biophys J. 2010; 99:2279–2288. [PubMed: 20923663] (b) Narayanan V, Scarlata S. Biochemistry. 2001; 40:9927–9934. [PubMed: 11502187]
- 13. Pfefferkorn CM, Lee JC. J Phys Chem B. 2010; 114:4615–4622. [PubMed: 20229987]
- 14. Lee JC, Langen R, Hummel PA, Gray HB, Winkler JR. Proc Natl Acad Sci USA. 2004; 101:16466–16471. [PubMed: 15536128]
- 15. Pfefferkorn CM, Jiang ZP, Lee JC. BBA-Biomembranes. 2012; 1818:162–171. [PubMed: 21819966]
- 16. Madine J, Doig AJ, Middleton DA. Biochemistry. 2006; 45:5783–5792. [PubMed: 16669622]
- 17. (a) Maltsev AS, Ying JF, Bax A. Biochemistry. 2012; 51:5004–5013. [PubMed: 22694188] (b) Kang LJ, Moriarty GM, Woods LA, Ashcroft AE, Radford SE, Baum J. Prot Sci. 2012; 21:911–017
- 18. Campelo F, McMahon HT, Kozlov MM. Biophys J. 2008; 95:2325–2339. [PubMed: 18515373]
- Stachowiak JC, Schmid EM, Ryan CJ, Ann HS, Sasaki DY, Sherman MB, Geissler PL, Fletcher DA, Hayden CC. Nat Cell Biol. 2012; 14:944–949. [PubMed: 22902598]
- 20. Thewalt JL, Bloom M. Biophys J. 1992; 63:1176–1181. [PubMed: 19431848]
- 21. Zhu M, Li J, Fink AL. J Biol Chem. 2003; 278:40186–40197. [PubMed: 12885775]
- 22. Uversky VN, Li J, Fink AL. J Biol Chem. 2001; 276:10737–10744. [PubMed: 11152691]
- Varkey J, Mizuno N, Hegde BG, Cheng N, Steven AC, Langen R. J Biol Chem. 2013; 288:17620– 17630. [PubMed: 23609437]
- 24. Lee JH, Hong CS, Lee S, Yang JE, Park YI, Lee D, Hyeon T, Jung S, Paik SR. Plos One. 2012:7.
- (a) Sorre B, Callan-Jones A, Manzi J, Goud B, Prost J, Bassereau P, Roux A. Proc Natl Acad Sci USA. 2012; 109:173–178. [PubMed: 22184226] (b) Yoon YD, Zhang XQ, Cho WH. J Biol Chem. 2012; 287:34078–34090. [PubMed: 22888025]
- 26. DeWitt DC, Rhoades E. Biochemistry. 2013; 52:2385–2387. [PubMed: 23528131]
- 27. (a) Alvarez-Erviti L, Seow Y, Schapira AH, Gardiner C, Sargent IL, Wood MJA, Cooper JM. Neurobiol Dis. 2011; 42:360–367. [PubMed: 21303699] (b) Danzer KM, Kranich LR, Ruf WP, Cagsal-Getkin O, Winslow AR, Zhu LY, Vanderburg CR, McLean PJ. Mol Neurodegen. 2012; 7:42.
- 28. (a) Emmanouilidou E, Melachroinou K, Roumeliotis T, Garbis SD, Ntzouni M, Margaritis LH, Stefanis L, Vekrellis K. J Neurosci. 2010; 30:6838–6851. [PubMed: 20484626] (b) Masuda-Suzukake M, Nonaka T, Hosokawa M, Oikawa T, Arai T, Akiyama H, Mann DMA, Hasegawa M. Brain. 2013; 136:1128–1138. [PubMed: 23466394]

29. (a) Giusto NM, Salvador GA, Castagnet PI, Pasquare SJ, de Boschero MGI. Neurochem Res. 2002; 27:1513–1523. [PubMed: 12512956] (b) Riekkinen P, Rinne UK, Pelliniemi TT, Sonninen V. Arch Neurol. 1975; 32:25–27. [PubMed: 1115656]

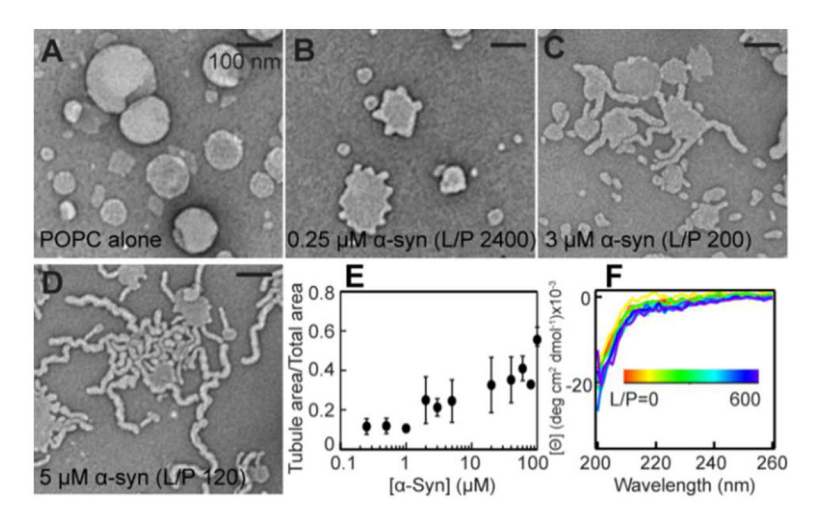


Figure 1. TEM images of POPC vesicle remodeling by α-syn. (A) POPC vesicles alone ([POPC] = 0.6 mM), (B) upon the addition of 0.25 μM, (C) 3 μM, and (D) 5 μM α-syn. Lipid-to-protein molar ratios (L/P) are as stated. Measurements were performed at RT. Length of scale bar is 100 nm. (E) Corresponding image analysis of tubule formation induced by increasing α-syn concentration. Mean values and standard deviations are shown. (F) CD spectra of α-syn (5 μM) as a function of increasing POPC concentration. (20 mM MOPS, 100 mM NaCl, pH 7, 25 °C). L/P (0–600) is colored from red to purple.

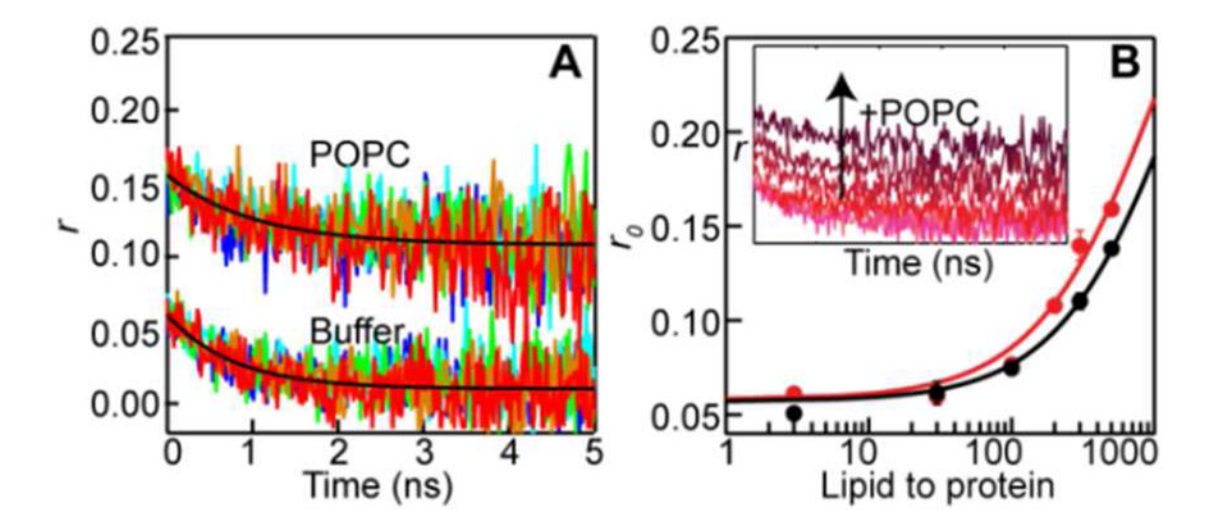
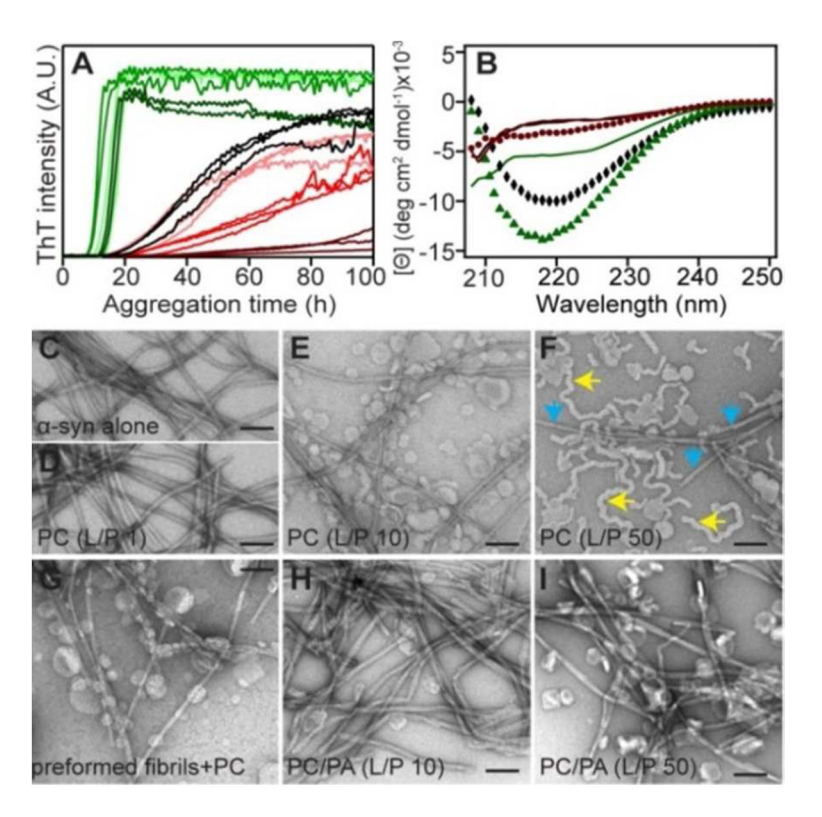


Figure 2. Time-resolved Trp anisotropy measurements. (**A**) Anisotropy (r) decays for F4W (blue), Y39W (cyan), F94W (green), Y125W (orange), and Y136W (red) in solution (5  $\mu$ M in 20 mM MOPS, 100 mM NaCl, pH 7, 25 °C) and upon the addition of POPC vesicles (1.5 mM). Representative single exponential fits are shown in black. See Figure S6 for N-acetyl-tryptophanamide controls. (**B**) Vesicle binding curves generated from F4W residual anisotropy ( $r_0$ ) for POPC (red) and POPC with 40% cholesterol (black). Error bars represent standard deviations from the mean for independent measurements. *Inset*: F4W anisotropy decays with increasing POPC vesicles (0 to 2.5 mM; L/P = 0–500). Labels for x- and y-axes are omitted for clarity.



**Figure 3.** α-Syn amyloid formation in the presence of lipid membranes. (**A**) Representative thioflavin T (ThT) fluorescence monitored aggregation kinetics for α-syn in solution (black) and with increasing POPC (light to dark red, L/P = 1, 10, and 50) and POPC/POPA (light to dark green, L/P = 1, 10, and 50) vesicles ([α-syn] = 70 μM in 20 mM MOPS, 100 mM NaCl, pH 7, 37 °C, orbital shaking, 2 mm glass beads). Data of replicates (n = 2-3) from one plate are shown. Lipid dependent trends were comparable and reproducible though variability in the absolute lag times was observed from different plates (n = 3). (**B**) Corresponding far-UV CD spectra for α-syn before (lines) and after (symbols) aggregation in buffer (black), with POPC (dark red, L/P = 50) and with POPC/POPA (dark green, L/P = 50). Representative TEM images for (**C**) α-syn in buffer, (**D**) α-syn + POPC (L/P = 1), (**E**) α-syn + POPC (L/P = 10), (**F**) α-syn + POPC (L/P = 50) after aggregation (4 d), cyan and yellow arrows indicate α-syn fibrils and membrane tubules, respectively, (**G**) POPC (0.6 mM) + preformed α-syn fibrils, (**H**) α-syn + POPC/POPA (L/P = 10), and (**I**) α-syn + POPC/POPA (L/P = 50) after aggregation (4 d). Length of scale bar is 100 nm.